

Noise thresholds for minimal surface code experiments

James R. Wootton, János R. Winkler and Daniel Loss

Department of Physics, University of Basel, Klingelbergstrasse 82, CH-4056 Basel, Switzerland

Current quantum technology is approaching the system sizes and fidelities required for quantum error correction. It is therefore important to determine exactly what is needed for proof-of-principle experiments, which will be the first major step towards fault-tolerant quantum computation. Here we propose an experiment using the smallest surface code that would allow errors to be detected and corrected for both the X and Z basis of a qubit. This requires 17 physical qubits initially prepared in a product state, on which 16 two-qubit entangling gates are applied before a final measurement of all qubits. Using a realistic error model, it is found that this set-up could successfully demonstrate error correction with two qubit gate fidelities greater than 91% and measurement fidelities greater than 96%. Fidelities of greater than 99%, however, are required to demonstrate a more convincing route to scalability.

PACS numbers: 03.67.Ac, 03.65.Vf, 03.67.Pp, 05.50.+q

INTRODUCTION

Quantum error correction is the set of methods required to manage noise in a quantum computer [1]. Before we can build a quantum computer we must first achieve quantum error correction, experimentally demonstrating that it can indeed correct quantum noise. In this paper we propose and study an experiment that could be used for this, and determine how low the noise levels must be in order for the experiment to succeed.

We consider the standard paradigm of quantum computation based on qubits: two level quantum systems [2]. A single ‘logical qubit’ is stored in a highly entangled two-dimensional subspace of a system of many ‘physical qubits’. The physical qubits experience unwanted influences, such as interactions with an environment, which are interpreted as noise. However, a logical qubit needs to experience arbitrarily low levels of noise in order to be useful within quantum computation. The multiqubit system is therefore defined such that the physical qubit noise cannot affect the logical qubit without leaving a measurable trace. By measuring a certain set of observables, known as stabilizers, these traces can be detected without affecting the logical qubit [3]. Such a set of measurement results is called the syndrome. Analysing this by means of a decoding algorithm determines how to remove the effects of the errors on the logical qubit. Sufficiently complex errors can overcome this strategy, and result in the attempted correction actually solidifying the effect of the error on the logical qubit. However, by extending the number of physical qubits used, the probability of this can be made vanishingly small.

EXPERIMENTAL DEVELOPMENT OF QUANTUM ERROR CORRECTION

We consider the experimental development of quantum error correction to consist of three distinct phases,

after which full development of fault-tolerant quantum computation can begin.

In the first phase, experiments will demonstrate necessary primitives for quantum error correction. This includes showing that the required states can be prepared [4], that the required entangling measurements can be made [5, 6] and demonstrating correction of a subset of the errors [5]. These experiments may also introduce artificial noise, to show the ability of the code to detect it [4, 6]. These experiments do not achieve quantum error correction themselves, but instead develop and demonstrate the necessary tools and techniques. This phase of development describes current experiments.

Future phases of proof-of-principle experiments will move on to larger codes (at least tens of qubits). They will use a complete set of syndrome measurements, capable of correcting all error types, and be operated at lower noise levels. This will allow them to fully achieve correction of the genuine noise experienced by the system.

We identify two future phases of such experiments. Phase 2 experiments will use only a single set of the required syndrome measurements before the final readout step. This is sufficient to detect and correct quantum errors in a way that will preserve the quantum information over a slightly longer time scale than usual.

In Phase 3 experiments the syndrome measurements will be repeated multiple times. This will allow quantum information to be preserved over much longer timescales. By using a number of measurement rounds that scales with system size, the lifetime should increase with system size also. This is the basis for arbitrarily increasing lifetime, as required for quantum computation.

Phase 2 experiments will be more straightforward than Phase 3 for several reasons. Firstly, the operations required for the syndrome measurement (entangling gates and ancilla measurements) need not be repeated. Secondly, the limited time frame in Phase 2 experiments allows less possibilities for logical errors to occur. The acceptable noise level will therefore be higher, and the

number of qubits required to suppress the errors will be lower. Phase 2 should therefore be the current priority, in order to build up the techniques needed for Phase 3. In this work, we propose an experiment that could begin the second phase.

MINIMAL SURFACE CODE

The proposed experiment considers the simplest non-trivial instance of the surface code method of quantum error correction [7]. It uses the smallest possible surface code that can both detect and correct quantum errors, which builds a single logical qubit from 9 physical qubits [8]. These are known as the code qubits. 8 stabilizer measurements are used to detect errors. Each is measured using an additional physical qubit that acts as an ancilla. A total of 17 physical qubits are therefore required. The code is shown in Figs. 1 and 2.

The stabilizers of this code can be defined in multiple different ways. Two are shown in Figs. 1(a) and 1(b). The former allows a more straightforward explanation of the proposed experiment, and so will be used for the following description.

The stabilizer observables, used to detect noise, are associated with plaquettes of the lattice. These plaquettes are split into two groups: white and blue. The white plaquettes are made up of σ_z operators. They therefore detect the effects of σ_x and σ_y errors, which we call bit flips. The blue plaquettes are made up of σ_x operators and detect the phase flips σ_z and σ_y . Note that σ_y is composed of both a bit and a phase flip, and so is detected by both types of stabilizer.

Though each individual σ_x operation anticommutes with some of the white plaquettes, a string across the code from left to right commutes with all. We associate any such operation with the Pauli operator X for the logical qubit. The eigenstates of these operators are therefore associated with the logical states $|+\rangle$ and $|-\rangle$. Similarly, a string of σ_z operations from top to bottom also commutes with all stabilizers and corresponds to the logical Z . Eigenstates of this are the logical qubit states $|0\rangle$ and $|1\rangle$.

Valid states of the logical qubit exist within the subspace that is the mutual $+1$ eigenspace of all stabilizers. Only highly entangled states exist within this space, and so their initialization will not be straightforward. However, consider the state for which all code qubits are $|0\rangle$. This is clearly in the $+1$ eigenspace of all white plaquette operators, and also for the logical Z operation. It can therefore be associated with the logical $|0\rangle$ state. It is nevertheless not an eigenstate of the blue plaquette operators. Measurement of these will therefore yield completely random results.

After the measurement of all stabilizers, the state will be forced into an mutual eigenstate of all stabilizers.

However, it will not be the mutual $+1$ eigenstate for the blue plaquettes, in general. To rectify this, σ_z operations could be applied to a subset of the code qubits such that the state is rotated to the mutual $+1$ eigenstate. There are many ways in which this can be done, which will differ from each other by a logical Z , with no clear indication of which is preferred. The procedure will therefore result in a logical Z being applied in error with high probability. However, since the initial logical state is $|0\rangle$, an eigenstate of Z , such an error would have no effect. We may therefore redefine our stabilizer space. Rather than the mutual $+1$ eigenstate of all plaquette operators, it will be the $+1$ eigenspace of blue plaquettes, and whatever eigenspace is obtained by the first set of measurements for the white plaquettes.

Similarly, the logical $|1\rangle$ state will be prepared when all code qubits are $|1\rangle$. The logical states $|+\rangle$ and $|-\rangle$ can also be prepared in a similar way, but the roles of the white and blue plaquettes will be interchanged.

In general, initialization will be followed by a period in which stabilizers are measured periodically for an arbitrarily long time. Also, manipulations required for quantum computation will be applied between measurement rounds. The effects of noise over time will be detected by the stabilizer measurements. Combined with the use of an arbitrarily large surface code (defined on an arbitrarily large grid), this process will allow the lifetime of the logical qubit to be made arbitrarily long.

Each round of syndrome measurement is done using a five-step transversal process. Firstly, each ancilla is paired with a unique code qubit, and an entangling gate is applied between each pair. For the blue plaquettes this will be a controlled-NOT, which either applies a σ_x or nothing to the ancilla depending on whether the code qubit state is $|1\rangle$ or $|0\rangle$, respectively. A similar gate is applied for the white plaquettes, but controlled on the $|+\rangle$ and $|-\rangle$ states of the code qubits. This process is then repeated three more times, so that each ancilla is entangled with each of its neighbouring code qubits.

The pairing of the qubits is done according to the numbering in Fig. 1(a), and the coloring of Fig. 2. The code qubit numbered 1 is entangled first for each stabilizer, and so on. The order is different for the two types of plaquette. This is to mitigate the effect of ancilla errors being spread to the code via the CNOTs, which can lead to uncorrectable errors if the ordering is not chosen carefully [8].

The ancilla qubits are initialized as $|0\rangle$. Their state after the application of the entangling gates then reflects the measurement results of the syndrome operators. The fifth and final step of the process is therefore to measure the ancilla qubits in the σ_z basis. The result $|0\rangle$ implies that the code lies within the $+1$ eigenspace of the corresponding stabilizer, and $|1\rangle$ implies the -1 eigenspace.

While the logical qubit is being stored, the syndrome measurements must be constantly repeated. The qubit

can then be read out by measuring in the logical Z or X basis. For the former, every code qubit is measured in the Z basis. This allows both the eigenstate of the logical Z operator and the blue plaquette stabilizers to be inferred. The latter provides a final syndrome measurement. The combination of all syndrome measurements can then be used to determine how to correct the output of the logical Z , in order to reflect the true state of the logical qubit.

The final syndrome measurement is different from standard ones in many important ways. Firstly, it can only be used to infer the measurement result for one type of plaquette: white plaquettes for Z measurements and blue for X . However, since this is always the type of plaquette required for correction of the measured basis, it does not pose any problem.

Also the fact that the code qubits are measured directly means that noisy measurements have a different effect. Specifically, noise that causes the measurement to report the wrong value has an equivalent effect to a bit flip (for Z measurements) applied directly before a perfect measurement. As such, we can consider this round to consist of perfect syndrome measurements, preceded by additional noise in the conjugate basis.

Since the ancilla qubits are not involved, there is another important difference. Standard syndrome measurements require use of the ancilla qubits at all points during the process: first for the entangling gates and then for measurement. There is therefore no scope to begin one round of measurements before previous one is finished. However, the code qubits are idle during the ancilla measurements. The readout measurements, which only involve code qubits, can therefore be performed concurrently with the ancilla measurements for the last standard syndrome round.

Finally, it is important to note that the readout measurements are not entangling. Applying readout directly after initialization would mean that the code never becomes entangled. At least one standard syndrome measurement is therefore required for the process to truly count as *quantum* error correction.

By using the stabilizers of Fig. 1(a), we treat bit and phase flip errors in a completely equivalent but independent way. Such an approach would be fine if both occur at the same rate. However, typically there are large differences between their noise levels. Dealing with them independently therefore means that our error correction will always be constrained by the noisier of the two.

This can be dealt with using the stabilizers of Fig. 1(b) [9]. These are equivalent to those of Fig. 1(a) up to local Hadamard rotations. All the analysis above therefore still applies, but with some exchanges between the σ_x and σ_z bases of code qubits. This will lead to both types of stabilizers detecting both types of errors (though still only one type per code qubit). The noisier form of error will then be corrected more effectively, since they are

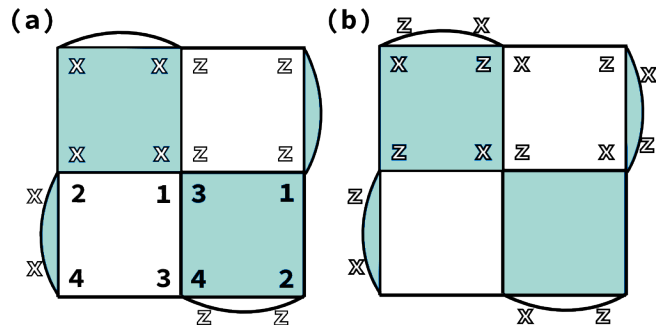


FIG. 1. Two alternative definitions of stabilizers in a surface code. Stabilizers are associated with plaquettes, including the four semi-oval plaquettes on the edges. Code qubits reside on the vertices of the lattices, and ancilla qubits reside on the center of each plaquette.

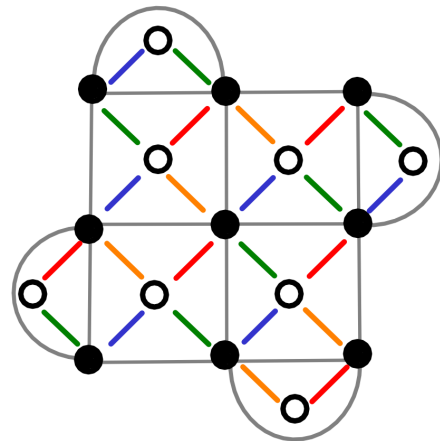


FIG. 2. Code qubits are shown with filled circles, and ancilla qubits with empty circles. The entangling gates are shown with colored lines. The red gates are performed first, followed by orange, then green and finally blue.

always mixed with the less noisy ones. As such, it is the stabilizers of Fig. 1(b) that we consider in our proposed experiment.

PROPOSED EXPERIMENT

For the simplest instance of surface code error correction, we need to implement the least number of syndrome measurement rounds. This means a single standard syndrome measurement is made, since any less would result in error correction that is not truly quantum.

The experiment will then consist of the following steps. First the physical qubits are initialized in the required product state. This will correspond to an initial logical state of $|0\rangle$, $|1\rangle$, $|+\rangle$ or $|-\rangle$. The four rounds of transversal entangling gates will then be applied, as in Fig 2. Finally, all physical qubits are measured. Ancil-

lae are measured in the σ_z basis, and each code qubit is measured in the σ_x or σ_z basis as required. Note that, since one type of stabilizer has random outcomes due to initialization and is not measured during readout, its results will not be used in the error correction process. Only the two rounds of results for the other syndrome type are used. Specifically, for a Z (X) measurement of the logical qubit we use only the outcomes of white (blue) stabilizers.

The basis chosen for readout of the logical qubit should always be the same as that of the initial state. With many samples, the fidelities of the states after error correction can then be determined.

For comparison, the same fidelity should also be determined for a single physical qubit. This allows us to assess the effectiveness of a code in protecting a logical qubit, in comparison with a logical qubit stored in a single physical qubit. It is only when this base level is improved upon that the error correction provides a benefit. It is then that the experiment can be deemed to be a success.

DECODING

Decoding is the process determining how best to correct errors given the syndrome results. For the surface code, this is typically done using approximate [8, 10, 11] or resource intensive algorithms [12]. In either case, the nature of the noise model must be known for the most effective decoding. However, due to the small size of the proposed set-up, the use of such algorithms can be avoided.

The experiment consists of two rounds of syndrome measurement, of which only four stabilizers in each contribute to error correction. This means that there are only $2^8 = 256$ possible sets of measurement outcomes. This allows us to perform decoding using a lookup table. Whenever we obtain a certain syndrome, we simply check the table to see whether keeping or flipping the readout logical value is more likely to give us the correct measurement result for the logical qubit.

The entries of this lookup table can be calculated using experimental data. The experiment can be run many times for different initial states. For each, the syndrome outcomes as well as the difference between the measured logical operator and the initial state is noted. The probability of the initial state being different to the measured logical operator can then be calculated for each syndrome value. With this data, we will know the best case strategy when we encounter each syndrome. Note that no theoretical assumptions about the noise required.

In our numerical studies, the lookup table is calculated using 10^5 samples.

NOISE MODEL

An important consideration for proof-of-principle experiments is how low the noise level must be. Our main focus is on determining noise levels that will allow the surface code to outperform a single physical qubit.

This will depend strongly on the size of the error correction problem, both in terms of code size and the number of measurement rounds. The thresholds determined for arbitrarily large codes and arbitrarily many rounds will therefore not apply to the case we consider. As such, we determine the threshold noise rates for success in this specific experiment.

Determining thresholds usually requires the application of a decoding algorithm to a large and representative set of noise samples. However, we are able to avoid this since we use a full look-up table decoder. Specifically, we use it to determine the probability of failed decoding for each syndrome, and sum these weighted by the probability of the syndromes. This results in the total probability of failure, and hence also the fidelity.

To determine the noise model to be considered, let us first consider the noise experienced by a single physical qubit that is not involved in a surface code. The fidelity with which this can store a logical qubit is the benchmark that the code must beat.

When preparing the physical qubit in the required initial state, $|0\rangle$, $|1\rangle$, $|+\rangle$ or $|-\rangle$, there will be some probability that this preparation fails. We model this as a perfect preparation followed by a bit flip with probability p_{bit} and a phase flip with probability p_{phase} . The former affects preparation of the σ_z basis states, swapping one for the other, and the latter affects the σ_x . For simplicity we will assume that $p_{bit} = p_{phase} = p$. The preparation fidelity is defined as $F_p = 1 - p$.

The qubit will then experience decoherence for a time t . For later convenience, we consider this as four successive periods of time $t/4$, the time for each entangling gate implemented in the surface code experiment. We consider the decoherence to be characterized by two timescales, T_1 and T_2 . The former is the timescale for amplitude damping, and the latter for dephasing. Approximating the effects of this noise using a Pauli channel gives σ_x , σ_y and σ_z errors with the following probabilities [8].

$$d_x = d_y = \frac{1 - e^{t/(4T_1)}}{4}, \quad d_z = \frac{1 - e^{t/(4T_2)}}{2} - p_x. \quad (1)$$

The fidelity for this decoherence process is defined as $F_{deco} = 1 - d_x - d_y - d_z$.

Finally, the qubit is measured in the σ_z or σ_x basis. This measurement will be imperfect, giving the opposite result with some probability. We model this as a perfect measurement preceded by a bit flip with probability m_{bit} and a phase flip with probability m_{phase} . The former leads to the incorrect outcome for a σ_z measurement, and

the latter for a σ_x measurement. For simplicity we will assume that $m_{bit} = m_{phase} = m$. The preparation fidelity is defined as $F_m = 1 - m$.

The total fidelity for this process is taken to be the probability that the qubit is measured in the same state in which it was prepared. This will yield two fidelities, F_{single}^z and F_{single}^x , for the two bases used. The overall fidelity is taken to be the minimum of these: $F_{single} = \min(F_{single}^z, F_{single}^x)$.

Now we consider the noise applied to physical qubits used within the surface code. As before, this begins with preparation noise and ends with measurement noise, as described above.

During the four rounds in which entangling gates are applied, the noise of these gates must be considered. We model this as depolarizing noise applied independently to the two qubits involved, prior to the application of a perfect gate. Each code and ancilla qubit is therefore subjected to four rounds of this noise. Exceptions are ancillae for two-qubit edge stabilizers. During rounds without entangling gates for these, they experience decoherence for the corresponding time $t/4$.

Unlike the noise considered previously, this does not apply bit and phase flips independently. It is therefore best described by application of the Pauli errors σ_x , σ_y and σ_z . The noise is independently applied to each qubit, with each Pauli error occurring with probability $g/3$. The probability that any one is applied is g .

The relationship between this probability and the fidelity of the gates depends on how this fidelity is defined. The form of the error here allows us to interpret the fidelity as the probability that no error is applied. This means $F_g = (1 - g)^2$.

The total fidelity for this process is again taken to be the probability that the logical qubit is measured in the same state in which it was prepared. This will yield two fidelities, F_{code}^z and F_{code}^x , for the two bases used. The overall fidelity is taken to be the minimum of these: $F_{code} = \min(F_{code}^z, F_{code}^x)$.

NUMERICAL RESULTS

Preliminaries

For the time scales, T_1 , T_2 and t , we note that the precise values do not matter, only their relative durations. All times are therefore stated in units of the T_2 time. The remaining free parameters are the timescales T_1/T_2 and t/T_2 , and the fidelities F_p , F_g and F_m .

With given values of these parameters, we can now simulate the noise and decoding to see whether or not the experiment would be successful in demonstrating quantum error correction. Specifically for fixed values of the

ratio T_1/T_2 , and of the ratio

$$f_m = \frac{1 - F_m}{1 - F_p}, \quad (2)$$

we find the lowest F_g that would lead to success (i.e. $F_{code} > F_{single}$) for various values of t and F_m . This is then repeated for different values of the ratios.

Results were taken for $T_1/T_2 \in \{10^2, 10^3, 10^4\}$ and $f_m \in \{1, 10\}$. The other parameters were considered in the form $t/T_2 = 10^{-a/2}$ and $F_g, F_m \in \{90\%, \dots, 99\%\}$.

In analyzing the data we will make use of the following ratio.

$$f_g = \frac{1 - F_g}{1 - F_{deco}^2}. \quad (3)$$

Here the numerator is the infidelity of two qubits acted upon by an entangling gate. The denominator is the infidelity of the same two qubits if simply left over the same time period to suffer from environmental decoherence. The value $f = 1$ therefore implies that the gate is effectively perfect and add no additional errors to that caused by environmental decoherence. For $f > 1$ the action of the gate adds additional noise.

Results

In all cases considered, the threshold for the measurement fidelity was in the range 94% – 98%. The higher end of this range was typical for $f_m = 1$ and the lower end for $f_m = 10$.

In all cases, the highest t/T_2 found was $1/\sqrt{10}$, and so approximately $t = T_2/3$. However, the price for this very long gate operation time is a threshold for gate fidelity such $f_g \approx 1$ (typically no higher than 1.21). The gate is therefore allowed to add very little additional noise in this case. More detailed dependence of f_g on t/T_2 is shown in Table I. Note f_g rises strongly as t/T_2 decreases, reaching $f_g \approx 40$ at $t/T_2 = 10^{-4}$ for $F_m = 99\%$. The same is also true as low as $F_m = 96\%$, in the case that $f_m = 10$.

The explicit values of the fidelity F_g varies from 90% to 99%. The former corresponds to the case of slow gates, and so the corresponding fidelity due to environmental noise would be a relatively low $F_{depol} = 92.5\%$. The $F_g = 99\%$ value corresponds to $t/T_2 \leq 10^{-2}$ and $F_{depol} \geq 99.8\%$.

The results suggest that the most experimentally accessible regime in which to run the experiment would be to have $F_m \geq 96\%$ and $F_p \geq 99.5\%$. The time required for an entire measurement round (four successive entangling gates) would be $t \leq T_2/\sqrt{10}$ with $T_1 \geq 100T_2$. The entangling gates would have fidelity $F_g > 91\%$.

This regime, however, benefits greatly from the comparative noise experienced by a single qubit. For a demonstration that is in line with scalability, measurement rounds of $t \leq T_2/100$ or $t \leq T_2/1000$ should be

t/T_2	$(10^2, 1)$	$(10^2, 10)$	$(10^3, 1)$	$(10^3, 10)$	$(10^4, 1)$	$(10^4, 10)$
0.316228	1.20083	1.20083	1.20633	1.34037	1.20689	1.34099
0.1	1.62199	2.02748	1.62933	2.03666	1.63006	2.03758
0.01	3.98755	3.98755	4.0055	8.011	4.0073	4.0073
0.001	39.8084	39.8084	39.9875	39.9875	40.0055	40.0055

TABLE I. This table shows the ratio f_g for various values of t/T_2 , T_1/T_2 and f_m for our optimal decoding scheme. The pairs of values on the top line are of the form $(T_1/T_2, f_m)$. All data here is for $F_m = 99\%$.

t/T_2	$(10^2, 1)$	$(10^2, 10)$	$(10^3, 1)$	$(10^3, 10)$	$(10^4, 1)$	$(10^4, 10)$
0.316228	1.0674	1.0674	1.0723	1.20633	1.20689	
0.1	1.62199	1.62199	1.62933	1.62933	1.63006	1.63006
0.01	3.98755	3.98755	4.0055	4.0055	4.0073	4.0073
0.001	39.8084	39.8084	39.9875	39.9875	40.0055	40.0055

TABLE II. This table shows the ratio f_g for various values of t/T_2 , T_1/T_2 and f_m for the decoding scheme of Tomita et al. The pairs of values on the top line are of the form $(T_1/T_2, f_m)$. All data here is for $F_m = 99\%$.

attempted. This results in a need for gate fidelities of $F_g > 99\%$. Nevertheless, for $f_m = 10$, the threshold for measurement fidelity remains at $F_m > 96\%$. For $F_p = F_m$, however, this rises to $F_m \geq 98\%$.

Intrinsic threshold estimates

Thresholds calculated in the standard fashion are defined for an arbitrarily large error correction problem [7]. But that is not the only way that they differ from the method used above. They also seek to determine the transition from noise levels that can be dealt with well by a code, to those that cannot. This is in contrast to the method above, which defines the threshold through comparison to an external system.

In order to gain additional information about the code and decoder that we use, it would be interesting to also calculate these threshold values. This requires data for a wide range of different system sizes. Our focus and the efficient applicability of our decoder, however, is limited to just a single system size. Nevertheless, we may still seek to learn something about these threshold values.

Calculation of thresholds typically requires many samples of noise to be randomly generated. Each such sample is prepared by first generating many random numbers, each of which take a value in the 0 to 1. These numbers are then compared to the probabilities for certain noise processes. If the random number is less than the probability with which it is compared, the corresponding element of the noise is said to have happened.

Each set of random numbers is typically used to generate only one noise sample. However, it has recently been found that using each for multiple samples can allow interesting new approaches [13]. Inspired by this, we use a

novel method based on a similar approach.

Explicitly, each set of random numbers will be used for multiple runs of the decoder. The noise for each set of random numbers will start at a low level, such that there will be no logical error in most cases. The noise is then progressively increased until the first time that a logical error arises. The value of the noise at this point is then noted. This gives us the notion of a threshold between correctability and non-correctability for the given set of random numbers.

This process is then repeated for many samples, each with a different set of random numbers. The average threshold noise rate is then determined. Due to the small system size, there can be expected to be a large range for different samples. To characterize this, the standard deviation is also calculated.

The noise parameters are chosen similarly to in the previous sections. However, due to the T_1 and T_2 times becoming far less prominent, we simply set $F_{depol} = 99.9\%$. The threshold F_g is then found for given values of F_m . The values of F_g used are from 79.9% to 99.9% in steps of 1%.

The results are shown in Fig. 3. It can be seen that these give far more lenient results than in the previous subsections. This should not come as a surprise, since this definition of the threshold basically finds the boundary between mostly succeeding and mostly failing. This is a lot less stringent a condition than needing to outperform a single qubit that suffers from no noisy entangling gates.

Comparison with other decoders

It is interesting to compare our decoding method to others that have been applied to the same code. The most obvious candidate is that of Tomita et al [8]. This is designed for repeated syndrome measurements, but can also be applied to our case. It is based on the application of a set of simple rules to simplify the syndrome and eventually determine whether the readout logical values should be changed. These rules are based on simple assumptions about the error model.

We find that the results obtained for the Tomita decoder are very similar to our optimal decoder for the noise model considered here. See the results of Table II. However, our decoder does show significant improvements for low t/T_2 and highly biased noise, which is likely the regime that will be used for the first experiments.

The lack of overall disagreement between the decoding methods is due to the assumptions made about noise for the Tomita decoder being true for the noise model we consider. For realistic systems, a larger disparity may be seen. Indeed, the lookup table obtained in experiments will be an important source of information about how noise affects the code. One metric that we can extract

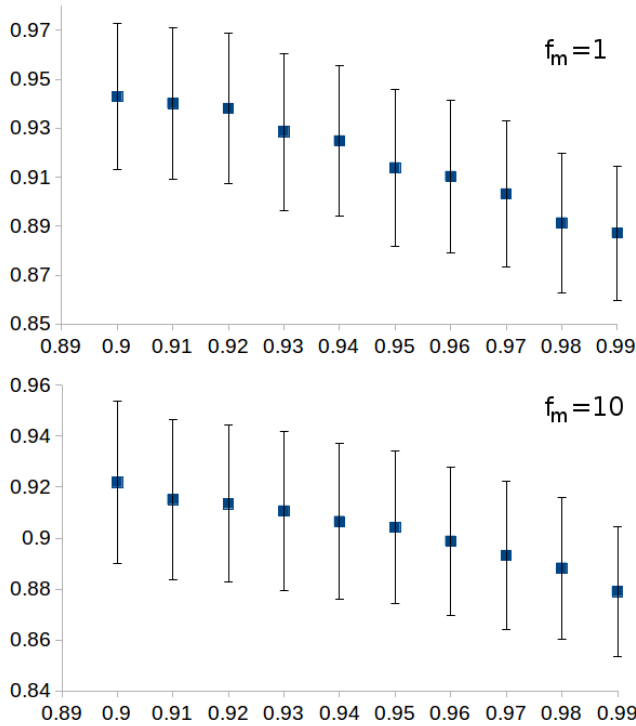


FIG. 3. Graphs of the threshold value of F_g against F_m . The points are the average values over 1000 samples, and the full width of each error bar is the standard deviation.

from this data is the difference between f_g for our decoder and that of Tomita et al, which characterises how far the noise is from typical theoretical models.

CONCLUSIONS

We have studied the simplest possible surface code experiment capable of demonstrating detection and correction quantum errors. With this we have determined the

noise levels required for this experiment to be a success, in terms of fidelities for the required operations, gate operation time and T_1 and T_2 time. The results constitute a concrete target for experimental noise levels, in systems proposed for quantum error correction.

The noise model used in our work is more realistic than those considered in many previous works (with [8] as a notable exception). However, there is much still to do in this direction. Noise models tailored to specific proposed set-ups will be considered in future work.

ACKNOWLEDGEMENTS

The authors would like to thank Christoph Kloeffer for discussions and the SNSF and NCCR QSIT for support.

-
- [1] D. A. Lidar and T. A. Brun, eds., *Quantum Error Correction* (Cambridge University Press, Cambridge, UK, 2013).
 - [2] M. A. Nielsen and I. L. Chuang, *Quantum Computation and Quantum Information* (Cambridge University Press, Cambridge, 2000).
 - [3] D. Gottesman, Phys. Rev. A **54**, 1862 (1996).
 - [4] D. Nigg, M. Müller, E. A. Martinez, P. Schindler, M. Hennrich, T. Monz, M. A. Martin-Delgado, and R. Blatt, Science **345**, 302 (2014).
 - [5] J. Kelly *et al.*, Nature **519**, 66 (2014).
 - [6] A. D. Corcoles *et al.*, Nature Communications **6** (2015).
 - [7] E. Dennis, A. Kitaev, A. Landahl, and J. Preskill, J. Math. Phys. **43**, 4452 (2002).
 - [8] Y. Tomita and K. M. Svore, Phys. Rev. A **90**, 062320 (2014).
 - [9] X.-G. Wen, Phys. Rev. Lett. **90**, 016803 (2003).
 - [10] A. G. Fowler and J. M. Martinis, Phys. Rev. A **89**, 032316 (2014).
 - [11] A. Hutter, J. R. Wootton, and D. Loss, Phys. Rev. A **89**, 022326 (2014).
 - [12] J. R. Wootton and D. Loss, Phys. Rev. Lett. **109**, 160503 (2012).
 - [13] C. Ferrie, S. Bartlett, and S. Flammia, in preparation.